Data Repository

The reliability of Vp or Vp/Vs anomaly changes is ensured if the resolution of the velocity models is consistent between the different epochs. To satisfy this requisite, we accurately selected the data, P- and S-wave arrival times and seismic stations to gain a more homogeneous volume sampling by seismic rays and verified ‘’a posteriori’’ the model resolution.

Data Selection

From the original dataset consisting of 2100 earthquakes, we selected earthquakes with hypocentral errors less than 1 km, rms location less than 0.3 s, azimuthal gap less than 180° and at least 18 seismic phases. Moreover, we optimize the volume sampling selecting those earthquakes that ensure a similar time spent at each node of the velocity model (similar Derivative Weight Sum). This requisite leads to the used epochs sub-division.

Details of the velocity inversions for the three epochs.

Epoch a (27/09-07-10) directly follows the two 26/09 mainshocks. A total of 6529 P-wave and 5940 S-P arrival times from 357 earthquakes are inverted achieving 75 % of the variance reduction and 0.08 s of the final rms, after 4 iterations.

Epoch b (07-10-17-10) encompasses the period during which the seismicity strongly migrated (figure 1). A total of 6348 P-wave and 5825 S-P arrival times from 364 earthquakes are inverted, achieving 71 % of the variance reduction and 0.08 s of the final rms after 4 iterations.

During Epoch c (18/10-03/11) seismicity is spread over the entire fault system. A total of 6590 P-wave and 6221 S-P arrival times from 451 earthquakes are inverted, achieving 82 % of the variance reduction and 0.08 s of the final rms after 4 iterations.

Resolution

For each epoch, we computed the full resolution matrix (R), following the approach of [De Gori et al., 2005]. The contribution of off-diagonal nodes in the estimation of each parameter is visualized by the spread function of R. For a node to be well resolved, the volume over which the velocity is estimated is centred to the node and the SF value is small. Supplementary figure. 1 shows the spread function and the DWS of the Vp/Vs model for the three epochs. We note that the region encompassing the 4D Vp/Vs variations is similarly resolved during the three epochs.

To further verify the reliability of anomaly change, we performed several synthetic tests using ‘’a priori’’ known heterogeneous models. P- and S-wave arrival times are computed tracing seismic rays through the synthetic model. They are inverted, after adding random noise, using the same model and parameters of the real inversion. We show results from one of those tests (Supplementary figure 2). Synthetic features are two high Vp/Vs anomalies located at 0 and 5 km depth and present in all the three epochs. We observe that anomaly 1 is well reproduced by the three epochs, and anomaly 2 is well reproduced in epochs b and c, while in epoch a is underestimated. The perturbation in nodes at the southern portion of the fault system is only slightly positive (+0.01) and not visible in the image. The resolution here is poor in epoch a, since seismicity migrated to the south only in periods b and c. Thus, the observed anomaly

changes are time-resolved for the whole period and only since October 7 in the central and southern part of the fault system, respectively.

Figure Captions

Supplementary Figure 1 Map of the spread function (grey coded scale and white contours) and DWS (contour line of 1000 in pink colour) for each epoch.

Supplementary Figure 2 Results of synthetic test for the three epochs. Two synthetic high Vp/Vs anomalies are located at the border of the central segment and on the southern segment, at 0 and 5 km depth, respectively. The synthetic features are consistently resolved by the three epochs.

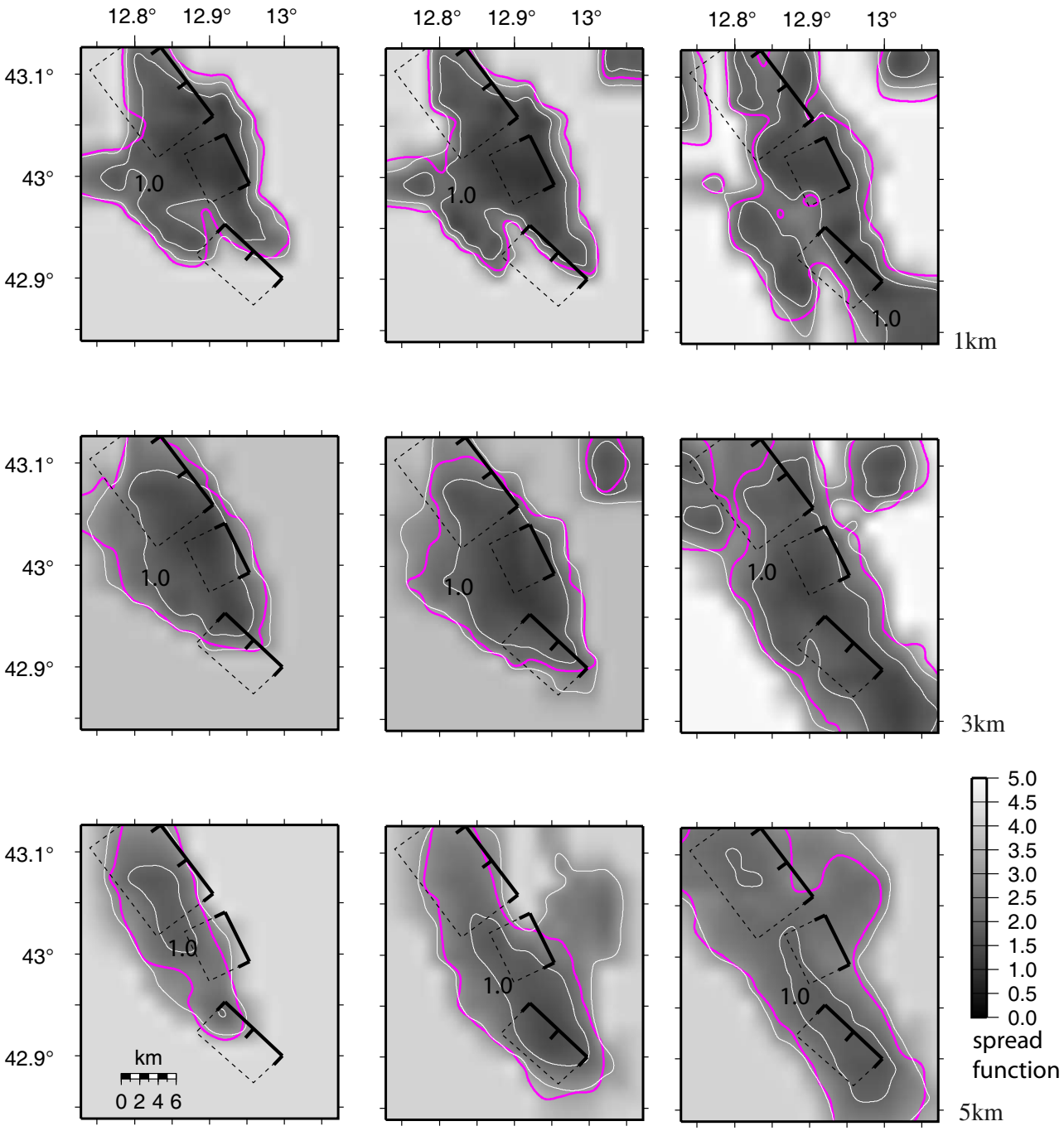

Supplementary Figure 1

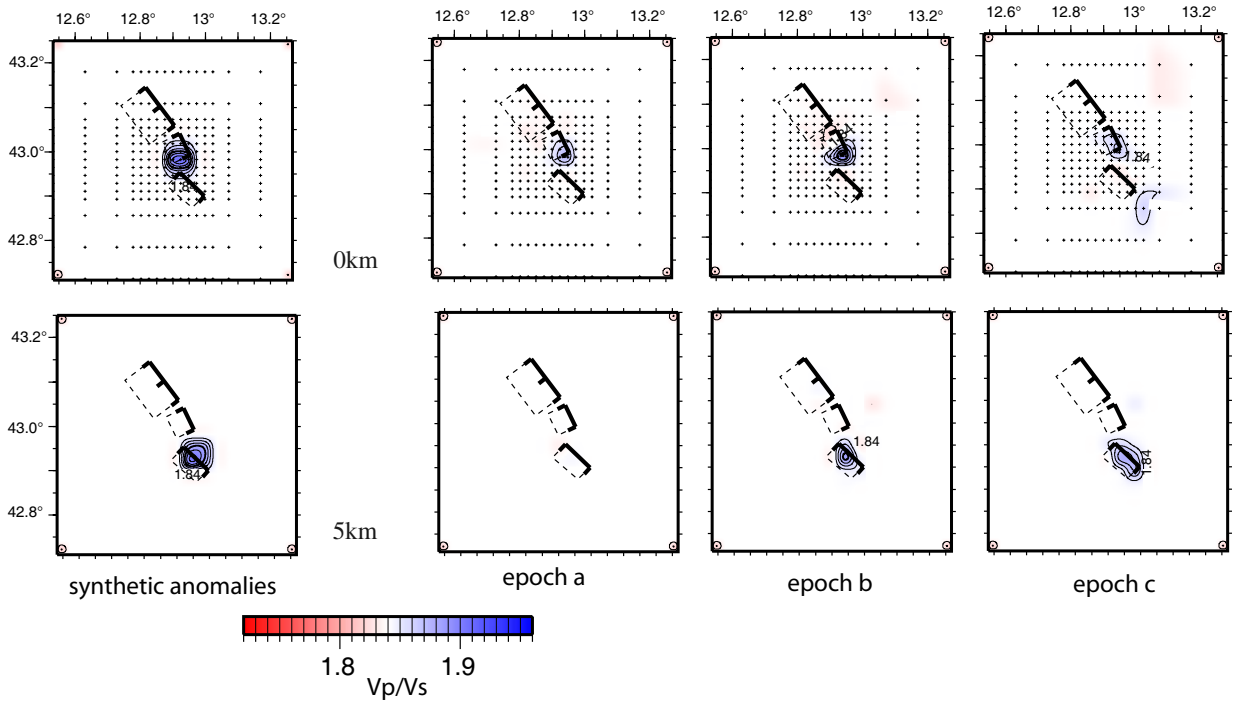

Supplementary Figure 2